

Cometary water expansion velocity from OH line shapes

W.-L. Tseng^{1,2}, D. Bockelée-Morvan¹, J. Crovisier¹, P. Colom¹, and W.-H. Ip²

¹ Observatoire de Paris, 5 place Jules Janssen, F-92195 Meudon, France

² Institute of Astronomy, National Central University, Chung Li 32054, Taiwan

Received 31 October, 2006; accepted 7 February 2007

ABSTRACT

Aims. We retrieve the H₂O expansion velocity in a number of comets, using the 18-cm line shapes of the OH radical observed with the Nançay radio telescope.

Methods. The H₂O velocity is derived from the large base of a trapezium fitted to the observed spectra. This method, which was previously applied to 9 comets, is now extended to 30 further comets. This allows us to study the evolution of their water molecule outflow velocity over a large range of heliocentric distances and gas production rates.

Results. Our analysis confirms and extends previous analyses. The retrieved expansion velocities increases with increasing gas production rates and decreasing heliocentric distances. Heuristic laws are proposed, which could be used for the interpretation of observations of cometary molecules and as a touchstone for hydrodynamical models. The expansion velocities retrieved from 18 cm line shapes are larger than those obtained from millimetric observations of parent molecules with smaller fields of view, which demonstrates the acceleration of the gas with cometocentric distance. Our results are in reasonable quantitative agreement with current hydrodynamical models of cometary atmospheres.

Key words. Comets: general – line: profiles – molecular processes – radio lines: Solar System

1. Introduction

Due to the small gravity field of cometary nuclei, cometary atmospheres are not captive and expand freely in the interplanetary medium. The expansion velocity of the atmosphere is a parameter of crucial importance for the interpretation of cometary observations and the modelling of cometary phenomena. This velocity is not constant; it is governed by the sublimation mechanism, photolytic heating of the coma and collisions, so that case-by-case studies are in principle necessary. It is suspected to depend basically upon the heliocentric distance, which governs photolytic heating, and the gas production rate, which governs collisions (e.g., Bockelée-Morvan & Crovisier 1987; Combi et al. 2005). Heuristic laws have been proposed, but they need to be checked and validated by hydrodynamical models and direct measurements.

One of the best methods to determine this expansion velocity is the observation of the shapes of molecular lines at radio wavelength, taking benefit of the high spectral resolution of such observation. These lines, when optically thin (which is practically the case for all species except water), have purely Doppler profiles. Therefore, they di-

rectly trace the velocity distribution over the line of sight. This has been applied to the millimetric and submillimetric lines of molecules, such as HCN, CO, CH₃OH, H₂S, directly sublimated from nucleus ices (e.g., Despois et al. 1986; Schloerb et al. 1987; Biver et al. 2002).

One can also use the OH lines at 18 cm, for which an important cometary database now exists. However, OH is a secondary species, coming from the photodissociation of water. At photodissociation, the OH radical is given an ejection velocity $V_d \approx 1 \text{ km s}^{-1}$ (Crovisier 1989). The kinematics and the space distribution of the OH radical must be evaluated in the frame of a *vectorial model* (Combi & Delsemme 1980; Festou 1981).

First attempts to deconvolve the OH line profiles in order to retrieve the expansion velocity V_p of the OH-parent used Monte Carlo simulations (Bockelée-Morvan & Gérard 1984; Tacconi-Garman et al. 1990). Another approach, proposed by Bockelée-Morvan et al. (1990, hereafter Paper I), derived the H₂O velocity from the large base of a trapezium fitted to the observed 18-cm line shapes of the OH radical. This method, which is much more rapid than Monte Carlo simulations, was applied to 9 comets observed with the Nançay radio telescope and checked over the Monte Carlo method in specific cases.

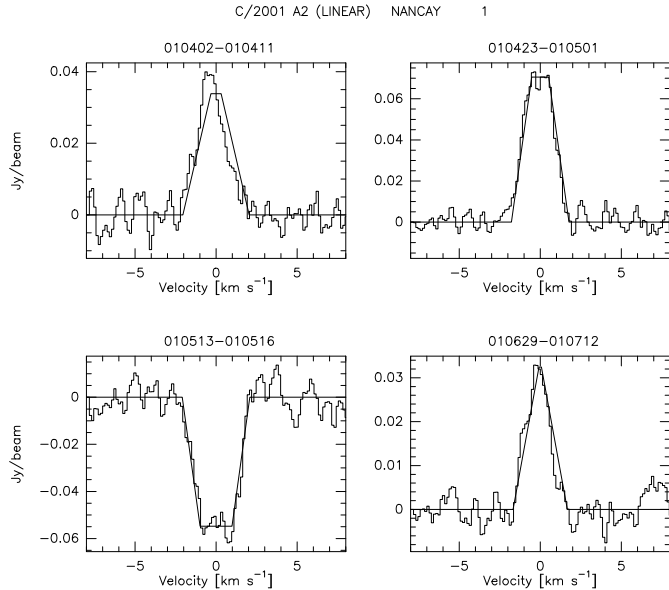


Fig. 1. A sample of OH spectra with their fitted trapezia: C/2001 A2 (LINEAR).

In the present paper, we extend this work to 30 further comets recently observed at Nançay, including C/1995 O1 (Hale-Bopp) which was observed up to more than 4 AU from the Sun, and several comets which were observed close (≈ 0.5 AU) to the Sun. This allows us to study the evolution of their water molecule outflow velocity over a wide range of heliocentric distances and gas production rates.

Section 2 presents the database and the method of analysis. Section 3 presents the results and the correlation between the gas expansion velocity, the heliocentric distance and the gas production rate. In Section 4, these results are discussed in the frame of hydrodynamical models of cometary atmospheres and are compared with other determinations of cometary expansion velocities. Section 5 concludes. Further details on this work are given in Tseng (2004).

2. Analysis

The database of OH observations of comets at Nançay up to 1999 is described in Crovisier et al. (2002a)¹. In 1995–2000, the Nançay radio telescope was upgraded (van Driel et al. 1996), resulting in improved performances of the instrumentation (the sensitivity was improved by a factor ≈ 2 and a more versatile spectrometer was installed). Cometary observations after this upgrade are described by Crovisier et al. (2002b, and in preparation). At 18 cm wavelength, the Nançay radio telescope has an elliptical field of view of $3.5' \times 19'$, which corresponds to $r_1 \times r_2 = 76\,000 \times 415\,000$ km at $\Delta = 1$ AU and is equivalent to a circular field of view of radius $r = \sqrt{r_1 r_2} = 178\,000$ km.

¹ See also

Table 1. Comets considered for the present analysis, listed by order of perihelion dates.

| Comet | N | ref. |
|------------------------------------|-----|------|
| C/1982 M1 Austin | 2 | a) |
| C/1984 N1 Austin | 2 | a) |
| 21P/Giacobini-Zinner (1985) | 5 | a) |
| C/1985 R1 Hartley-Good | 4 | a) |
| C/1985 T1 Thiele | 1 | a) |
| 1P/1982 U1 Halley | 26 | a) |
| C/1986 V1 Sorrells | 1 | a) |
| C/1986 P1 Wilson | 13 | a) |
| C/1987 P1 Bradfield | 3 | a) |
| C/1990 K1 Levy | 15 | b) |
| 109P/1992 S2 Swift-Tuttle | 10 | c) |
| C/1988 A1 Liller | 1 | d) |
| 23P/1989 N1 Brorsen-Metcalf | 2 | d) |
| C/1989 Q1 Okazaki-Levy-Rudenko | 2 | d) |
| C/1989 W1 Aarseth-Brewington | 1 | d) |
| C/1989 X1 Austin | 3 | d) |
| C/1991 Y1 Zanotta-Brewington | 1 | d) |
| C/1991 T2 Shoemaker-Levy | 1 | d) |
| 24P/Schaumasse (1993) | 1 | d) |
| C/1993 Y1 McNaught-Russell | 1 | d) |
| 19P/Borrelly (1994, 2001) | 8 | d) |
| 45P/Honda-Mrkos-Pajdušáková (1996) | 1 | d) |
| C/1996 B2 Hyakutake | 9 | d) |
| 22P/Kopff (1996) | 2 | d) |
| C/1996 Q1 Tabur | 1 | d) |
| C/1995 O1 Hale-Bopp | 28 | d) |
| C/1998 J1 SOHO | 1 | d) |
| 21P/Giacobini-Zinner (1998) | 2 | d) |
| C/1999 H1 Lee | 7 | d) |
| C/1999 N2 Lynn | 1 | d) |
| C/1999 T1 McNaught-Hartley | 3 | d) |
| C/2000 W1 Utsunomiya-Jones | 1 | d) |
| C/2001 A2 LINEAR | 9 | d) |
| C/2000 WM ₁ LINEAR | 3 | d) |
| 153P/2002 C1 Ikeya-Zhang | 8 | d) |
| C/2002 F1 Utsunomiya | 2 | d) |
| C/2002 V1 NEAT | 6 | d) |
| C/2002 X5 Kudo-Fujikawa | 3 | d) |
| C/2002 Y1 Juels-Holvorcem | 3 | d) |

N is the number of samples for each comet.

- a) Bockelée-Morvan et al. (1990).
- b) Bockelée-Morvan et al. (1992).
- c) Bockelée-Morvan et al. (1994).
- d) Present work.

As explained in Paper I, a symmetric trapezium is fitted to the OH line. The large base of the trapezium is assumed to be $2(V_p + V_d)$, where V_p is the water expansion velocity and V_d is the OH ejection velocity upon water photodissociation. As discussed in Paper I, we assume $V_d = 0.9$ km s⁻¹, which is close to the theoretical value of 1.05 km s⁻¹ (Crovisier 1989). Hence the evaluation of V_p . An example of OH spectra with their fitted trapezia is shown in Fig. 1.

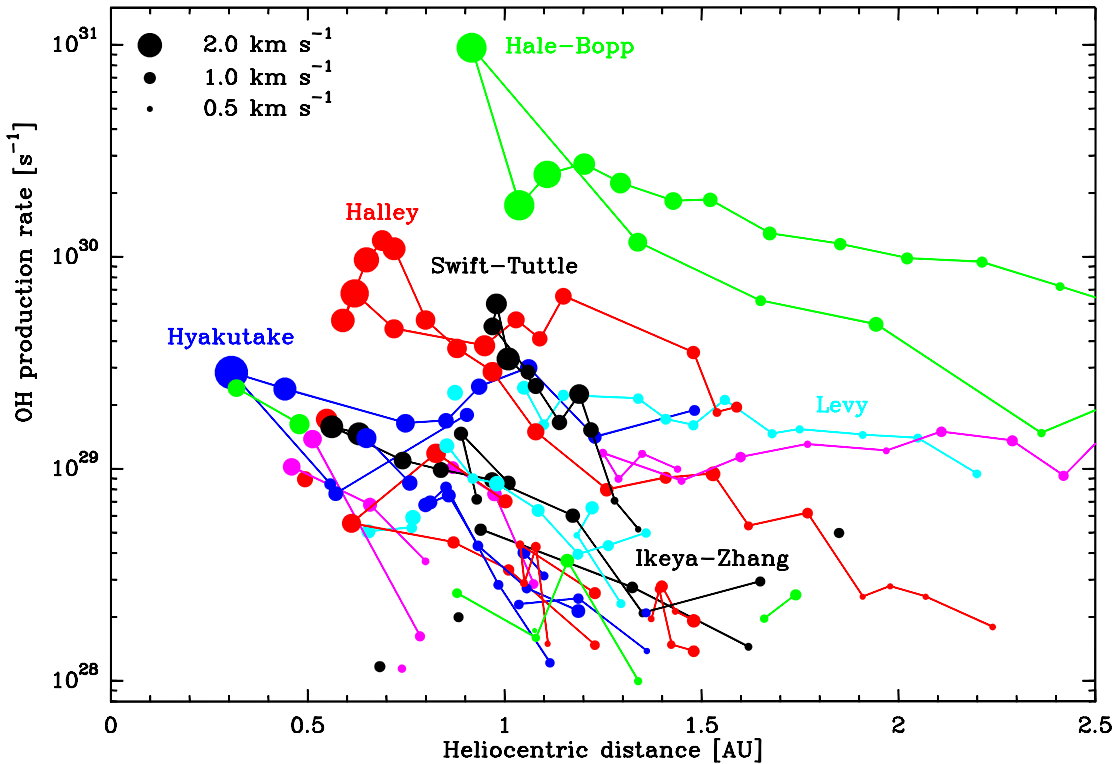


Fig. 3. Correlation between the retrieved water expansion velocity V_p , heliocentric distance r_h , and OH production rate Q_{OH} . The size of each circle is proportional to V_p . The well-studied comets 1P/Halley, C/1990 K1 (Levy), 109P/Swift-Tuttle, C/1996 B2 (Hyakutake), C/1995 O1 (Hale-Bopp) and 153P/2002 C1 (Ikeya-Zhang) are identified by their names.

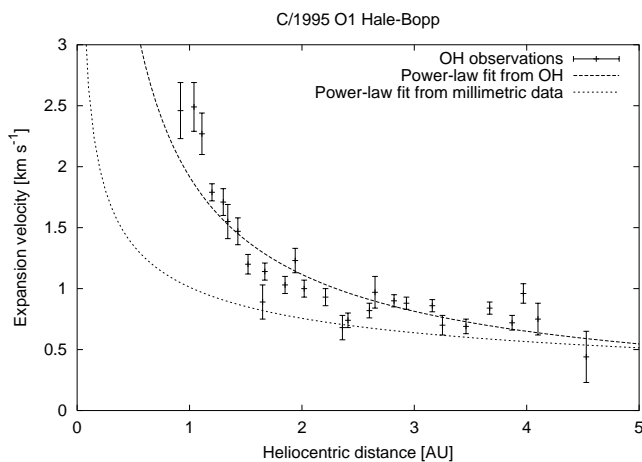


Fig. 2. Evolution of the expansion velocity V_p as a function of heliocentric distance r_h for C/1995 O1 (Hale-Bopp). Pre-perihelion and post-perihelion data are combined. The dashed line shows the power-law fit (Eq. 1) to the OH data. The dotted line shows the power-law fit (Eq. 2) to the velocities derived from the millimetric molecular lines (Biver et al. 2002).

As in Paper I, the OH production rates Q_{OH} are derived using the OH inversion curve of Despois et al. (1981) and the quenching law and OH parameters of Gérard (1990). The model is fully described in Crovisier et al. (2002a, Table 3, last column). The model consistently uses the parent velocity derived from the trapezium fit to compute the OH production rate; therefore, the production rates of the present analysis may differ somewhat from those published by Crovisier et al. (2002a) which were computed assuming $V_p = 0.8 \text{ km s}^{-1}$.

The list of comets investigated in the present study is given in Table 1. The analysis is performed on spectra integrated over several days for which the signal-to-noise ratio is sufficient (typically > 10). The total number of samples is 190. A comprehensive tabulation of the data may be found in Tseng (2004).

As an example, the expansion velocity as a function of heliocentric distance r_h is shown in Fig. 2 for C/1995 O1 (Hale-Bopp), for which the OH lines could be observed over a large range of r_h . The fitted power law is

$$V_p = 1.917(\pm 0.055)r_h^{-0.78(\pm 0.04)} \text{ km s}^{-1}, \quad (1)$$

to be compared to

$$V_p = 1.125(\pm 0.015)r_h^{-0.42(\pm 0.01)} \text{ km s}^{-1} \quad (2)$$

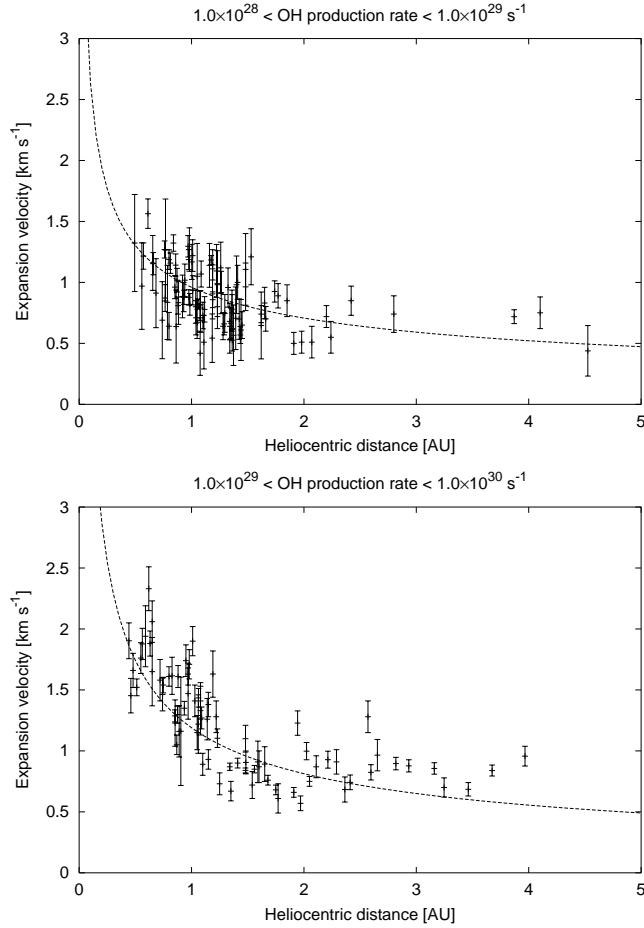


Fig. 4. Evolution of the expansion velocity V_p as a function of heliocentric distance r_h for given Q_{OH} ranges. The fitted power laws are listed in Table 2.

for the velocities derived from the millimetric molecular lines (Biver et al. 2002) which were observed in a smaller field of view (see discussion in Section 4). One must note that in the range $0.92 < r_h < 4.57$ AU which is investigated here, Q_{OH} varied by about three orders of magnitude, so that the strong variation on r_h implicitly includes a dependence on both r_h and Q_{OH} .

3. Results

From the profiles of the 18-cm OH lines, we have investigated the expansion velocity V_p of cometary atmospheres for heliocentric distances r_h ranging from 0.3 to 4.6 AU and OH production rates Q_{OH} from 10^{28} to 10^{31} s^{-1} . Confirming the results of Paper I, V_p is found to consistently increase with increasing Q_{OH} and with decreasing r_h , as expected qualitatively from hydrodynamical models (Combi et al. 2005 and references therein). The observed V_p 's range from 0.5 to 2.5 km s^{-1} .

An overview of the correlation between retrieved water expansion velocities, heliocentric distances and OH production rates is shown in Fig. 3 (an update of Fig. 14 in Paper I). In order to investigate separately the dependence

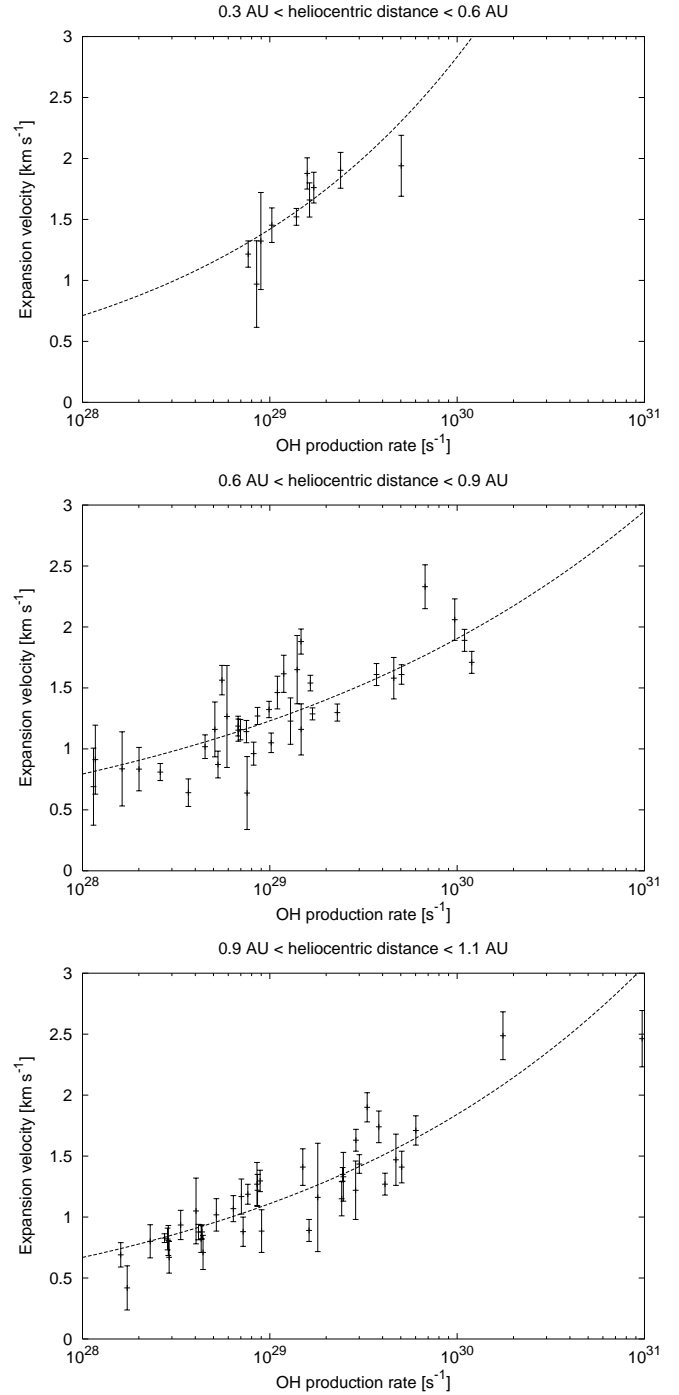


Fig. 5. Evolution of the expansion velocity V_p as a function of Q_{OH} for given heliocentric distance (r_h) ranges. The fitted power laws are listed in Table 2.

of V_p to r_h and Q_{OH} , we have divided the data into various subsamples. Power laws fitted to the different subsamples are listed in Table 2 and shown in Figs 4–5.

From these plots, we can see the existence of a threshold effect: the expansion velocities are ≈ 0.8 km s^{-1} , insensitive to the heliocentric distances from 1.5 to 5.0 AU for moderately active comets with OH production rates from a few 10^{28} s^{-1} to a few 10^{29} s^{-1} . The expansion ve-

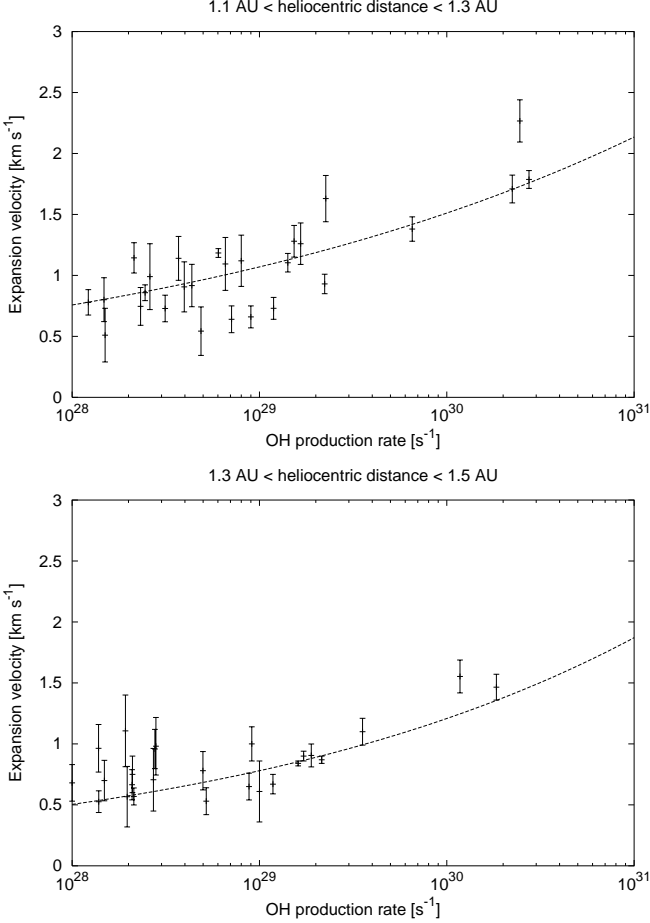


Fig. 5. (continued)

locities strongly depend on the heliocentric distance for $r_h \leq 1.5$ AU.

Errors reported in Table 2 are the $1-\sigma$ formal errors resulting from the fits to the data. They do not include

Table 2. Power-law fits to the H_2O expansion velocity V_p (in km s^{-1}) obtained from the OH radio observations at Nançay for different ranges of production rates Q_{OH} and heliocentric distances r_h . The corresponding data with plots of the fitted power laws are shown in Figs 4–5.

| Q_{OH} range [s^{-1}] | power-law fit [r_h in units of AU] |
|--|---|
| $10^{28} - 10^{29}$ | $V_p = 0.96 \pm 0.01 \times r_h^{-0.44 \pm 0.04}$ |
| $10^{29} - 10^{30}$ | $V_p = 1.19 \pm 0.01 \times r_h^{-0.55 \pm 0.02}$ |
| r_h range [AU] | power-law fit [Q_{OH} in units of 10^{29} s^{-1}] |
| 0.3 – 0.6 | $V_p = 1.42 \pm 0.05 \times Q_{\text{OH}}^{0.30 \pm 0.06}$ |
| 0.6 – 0.9 | $V_p = 1.23 \pm 0.02 \times Q_{\text{OH}}^{0.19 \pm 0.01}$ |
| 0.9 – 1.1 | $V_p = 1.11 \pm 0.02 \times Q_{\text{OH}}^{0.22 \pm 0.01}$ |
| 1.1 – 1.3 | $V_p = 1.07 \pm 0.02 \times Q_{\text{OH}}^{0.15 \pm 0.01}$ |
| 1.3 – 1.5 | $V_p = 0.78 \pm 0.02 \times Q_{\text{OH}}^{0.19 \pm 0.02}$ |

possible systematic errors due to shortcomings in the modelling. Given the limited number of data, their arbitrary binning, and possible systematic effects, we do not think that the differences of the exponent of the power law r_h^α , in the upper part of Table 2, are firmly established. The same for the exponent of Q_{OH}^β in the lower part of the table. $\alpha = -0.5$ and $\beta = 0.2$ are probably the values to be retained.

Taking a step further, we tried to fit a combined power law $r_h^\alpha Q_{\text{OH}}^\beta$ to our data. A unique law could not be obtained for the whole domain covered by the observations. The results are shown in Table 3. For $r_h > 2$ AU, V_p barely depends upon r_h and Q_{OH} as already discussed. The dependence with Q_{OH} is $\propto Q_{\text{OH}}^{0.20}$ over the range 0.3–2 AU, as inferred from Q_{OH} power-law fits over restricted ranges of r_h (Table 2). Between 0.3 and 1 AU, the r_h dependence is in $r_h^{-0.45}$, but the data suggest a steeper heliocentric dependence in r_h^{-1} between 1 and 2 AU. Power-law fits in the subsamples [$10^{28} < Q_{\text{OH}} < 10^{29} \text{ s}^{-1}$; $1 < r_h < 1.5$ AU] and [$10^{29} < Q_{\text{OH}} < 10^{31} \text{ s}^{-1}$; $1 < r_h < 2$ AU] are similar ($\sim Q_{\text{OH}}^{0.20} r_h^{-1}$), which suggests that the difference in heliocentric evolution between $r_h < 1$ AU and $r_h > 1$ AU could be a characteristics of V_p behaviour. Note, however, that there is significant dispersion between the data and the fitted curves (reduced χ^2 between 2 and 3, see Table 3).

4. Discussion

The empirical laws derived from non-linear fits and listed in Table 2 can be used as a touchstone for hydrodynamical models of cometary atmospheres. They can also help us to analyse cometary observations, and especially to derive more reliable OH production rates from the 18-cm observations, when the signal-to-noise ratio is not sufficient to apply the trapezium method to the line shapes.

These results, however, should only be used for the range of parameters (r_h , Q_{OH}) pertaining to the data analysed in the present work. In particular, we caution the reader against extrapolating the laws of Table 2 to distant comets. At large r_h 's, cometary activity is governed by the sublimation of CO and other hypervolatile species rather than that of water, resulting in quite different temperatures and velocities at the nucleus surface (Ip 1983).

The top part of Table 2 shows that, for a restricted range of Q_{OH} , the heliocentric dependence is close to the law

$$V_p = 0.85 \times r_h^{-0.5} \text{ km s}^{-1} \quad (3)$$

which was proposed sometime (e.g., Cochran & Schleicher 1993; Budzien et al. 1994). But the dependence upon Q_{OH} cannot be ignored. Cochran & Schleicher (1993) proposed the law

$$V_p = 0.7 + 1.3 \times Q_{\text{H}_2\text{O}}^{0.5} \text{ km s}^{-1} \quad (4)$$

for $r_h \approx 1$ AU from the results of Paper I, where $Q_{\text{H}_2\text{O}}$ is in units of 10^{30} s^{-1} . This law appears to be a poor fit to our data.

Table 3. Combined r_h and Q_{OH} power-law fits to the expansion velocity V_p (in km s^{-1}) for different ranges of Q_{OH} and heliocentric distance.

| r_h range [AU] | Q_{OH} range [s^{-1}] | combined power-law fit [Q_{OH} in units of 10^{29} s^{-1}] | reduced χ^2 |
|---------------------|--|--|------------------|
| $0.3 < r_h < 1.0$ | $10^{28} < Q_{\text{OH}} < 10^{30}$ | $V_p = 1.11 \pm 0.02 \times r_h^{-0.45 \pm 0.05} \times Q_{\text{OH}}^{0.23 \pm 0.01}$ | 2.0 |
| $1.0 < r_h < 2.0$ | $10^{28} < Q_{\text{OH}} < 10^{31}$ | $V_p = 1.17 \pm 0.02 \times r_h^{-0.99 \pm 0.05} \times Q_{\text{OH}}^{0.18 \pm 0.01}$ | 3.3 |
| $2.0 < r_h < 4.6$ | $10^{28} < Q_{\text{OH}} < 10^{30}$ | $V_p = 0.71 \pm 0.02 \times r_h^{-0.07 \pm 0.08} \times Q_{\text{OH}}^{0.09 \pm 0.02}$ | 2.0 |

Interestingly, photochemical heating is more sensitive to the heliocentric distance than to the water production rate. The heating rate is directly proportional to r_h^{-2} (through the water photodissociation rate), but is weighted by the efficiency of the thermalization process of fast hydrogens. The size of the region where the efficiency is significant scales proportionally to the water production rate (e.g., Ip 1983; Bockelée-Morvan & Crovisier 1987). Though other processes, such as radiative cooling, do affect the hydrodynamics of the coma, the steeper r_h dependency (compared to Q_{OH} variation) observed in our data is consistent with photolytic heating being the main process controlling the gas velocity in the outer coma. The different heliocentric variations in the 0.3–1 AU and 1–2 AU domains remain to be explained.

We will now compare our results with other observations and with model predictions. For this prospect, we have to take into account the effect of the field of view and of the geocentric distance Δ .

The *expansion velocity* of a cometary atmosphere is not a well defined parameter. In the inner, collisional coma where classical hydrodynamics prevails, this velocity is progressively increasing with distance r to the nucleus, as a result of photolytic heating (Combi et al. 2005). In the outer coma where the free-molecular flow is governed by rarefied gas dynamics, the velocity distribution is not maxwellian.

The observed line shapes are averages of all molecules present in the instrumental field of view. In the following, we will assume that the observed V_p is representative of molecules at a distance r equal to the field-of-view radius. This assumption is justified by Monte Carlo simulations of the HCN line shape (Paper I, Fig. 15). Alternatively, the field of view radius for 18-cm observations may be larger than the water scale length l_p for photodissociation (typically $l_p \approx 10^5$ km at 1 AU). In this case, we may wish to adopt $r = l_p$. This must be considered as an approximation.

We note that one would also expect that for very small fields of view, the collisional region is sampled, in which OH is thermalized and partakes the kinetics of water. Then the trapezium model would fail. An extreme observational case was that of comet C/1996 B2 (Hyakutake), which was observed at $r_h = 1.06$ AU, $\Delta = 0.13$ AU, with $Q_{\text{OH}} \approx 3 \times 10^{29} \text{ s}^{-1}$. We retrieved $V_p = 1.4 \text{ km s}^{-1}$, right in the range of the laws of Table 2. Quite recently, we observed 73P/Schwassmann-Wachmann 3 at $\Delta = 0.08$ AU

only, with $r_h = 1.0$ AU and $Q_{\text{OH}} \approx 10^{28} \text{ s}^{-1}$; the retrieved V_p (0.8 km s^{-1}) was also *normal* (Crovisier et al., in preparation; these observations are not in the database analysed in the present work). This suggests that for both observations, the field of view was still not small enough for a significant thermalization of the OH radicals, or that this thermalization also quenched the OH maser, so that the 18 cm observations are insensitive to such OH radicals.

Complementary data are provided by millimetric and submillimetric observations of line shapes of parent molecules. V_p is then close to the line half-width at half maximum (Biver et al. 2002 adopt for V_p 90% of the half-width, to account for thermal broadening). Data for several molecules (especially HCN, CO, CH_3OH and H_2S) are now available for many comets (e.g., observations at IRAM, SEST, JCMT and CSO; Biver et al. 1999, 2000, 2002, 2006). Direct observations of the water line at 557 GHz from space with the *SWAS* and *Odin* satellites also exist (Neufeld et al. 2000; Lecacheux et al. 2003), but their kinematic interpretation is hampered by the saturation of this strong line.

The typical angular field-of-view diameter for millimetric observations with the IRAM 30-m telescope is $17''$ at a frequency of 145 GHz, corresponding to a linear radius $r = 6200$ km at a geocentric distance $\Delta = 1$ AU. This is much smaller than the elliptical field of view of the Nançay radio telescope (equivalent to a radius of 178 000 km).

As previously noted in, e.g., Paper I, the V_p determined from parent molecules observed at millimetric wavelengths are systematically smaller than those obtained from OH line shapes, with larger fields of view. This effect is shown in Fig. 6. Observations of comets 1P/Halley, C/1996 B2 (Hyakutake), C/1995 O1 (Hale-Bopp), C/1999 H1 (Lee) and 153P/2002 C1 (Ikeya-Zhang) were selected at various r_h 's, chosen so that the gas production rates were similar (Q_{OH} in the range $1\text{--}4 \times 10^{29} \text{ s}^{-1}$). Points on the right are V_p determined from the present work. Points on the left are measurements from millimetric observations (Biver et al. 1999, 2000, 2002, 2006). For comet Halley, the various points from left to right are from in situ measurements (*Giotto*, Lämmerzahl et al. 1987), HCN (IRAM, Despois et al. 1986), HCN (FCRAO, Schloerb et al. 1987) and OH (Nançay, present work). As discussed above, r is evaluated as the field-of-view radius. For all comets, an increase of V_p with r is observed. This increase is much more important for comets close to the Sun (e.g., 153P/2002 C1 (Ikeya-Zhang) at $r_h = 0.6$ AU) than for

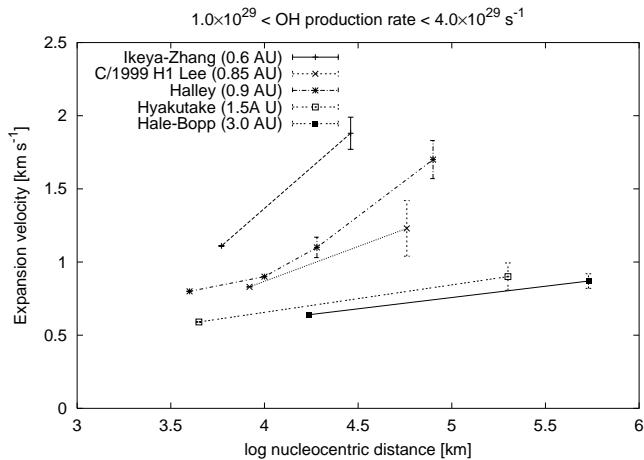


Fig. 6. Field-of-view effects demonstrating the acceleration of the gas. V_p determined from the present work (right-hand points) or from millimetric observations (left-hand points) is plotted as a function of the cometocentric distance r corresponding to the field of view. See text for details.

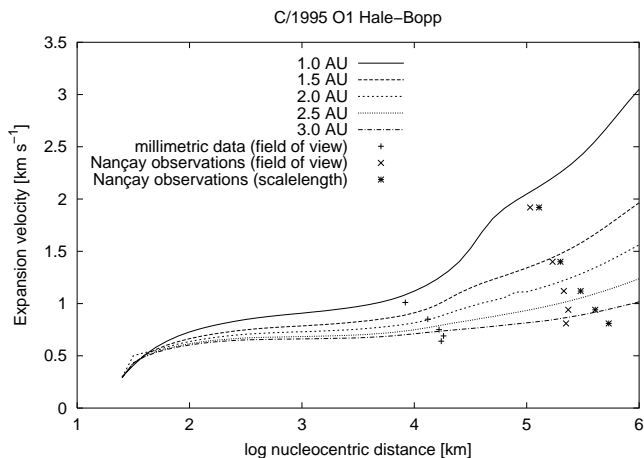


Fig. 7. Model predictions of V_p as a function of cometocentric distance, for comet C/1995 O1 (Hale-Bopp) pre-perihelion, adapted from Fig. 1 of Combi et al. (1999). Observational determinations have been superimposed. See text for details.

distant comets (e.g., C/1995 O1 (Hale-Bopp) at 3 AU). This clearly demonstrates the acceleration of the gas with cometocentric distance, attributed to photolytic heating.

Direct imaging of near-UV OH emission was made by Harris et al. (2002) in comet C/1995 O1 (Hale-Bopp). From their analysis, $V_p = 2.3 \text{ km s}^{-1}$ was retrieved for $Q_{\text{OH}} \approx 10^{31} \text{ s}^{-1}$ for cometocentric distances $\approx 10^6 \text{ km}$. This agrees well with our measurement (2.4 km s^{-1}).

In order to achieve a quantitative comparison of these results with models, we have plotted in Fig. 7 the predictions of the hybrid kinetic/dusty gas hydrodynamical model of Combi et al. (1999) for comet C/1995 O1 (Hale-Bopp). V_p as a function of cometocentric distance is plotted for five heliocentric distances (1.0, 1.5, 2.0, 2.5 and

3.0 AU, all pre-perihelion) and the corresponding observed water production rates ($80, 20, 14, 4$ and $4 \times 10^{29} \text{ s}^{-1}$, respectively, according to Combi et al.). Observational determinations of V_p , from the present work (points on the right) and from the millimetric observations of Biver et al. (2002) (points on the left), have been superimposed. For all these points, the cometocentric distances are again those corresponding to the field-of-view radii. We can see that the model predictions lead to somewhat overestimated velocities. Otherwise, the variation of V_p with r and r_h (and the related Q_{OH}) is remarkably well reproduced by the model. The discrepancy between model and observations may be attributed to:

- flaws in the modelling of the heating/cooling processes (one can note that the model of Combi et al. (1999) also predicts temperatures higher than those observed by Biver et al. 2002);
- the difficulty to model the transitional region between hydrodynamical flow and free-molecular flow (sophisticated Monte Carlo simulations are required; cf. Hodges 1990);
- an inaccurate estimation of the cometocentric distance to which the measured V_p pertains (see discussion above);
- the presence of anisotropic outgassing, whereas models assume spherical symmetry.

Finally, we note that, as already discussed in Paper I, there are some observations, especially for distant, weak comets, leading to small values of V_p ($0.5\text{--}0.6 \text{ km s}^{-1}$) that can difficultly be reconciled with hydrodynamical models.

5. Conclusion

We have extended the previous analysis of OH 18-cm line shapes from the Nançay database (paper I) from 9 to 39 comets with the following results:

- This analysis confirms the increase of the coma expansion velocity V_p with increasing gas production rate Q_{OH} and decreasing heliocentric distance r_h .
- The results are summarized in Tables 2 and 3 which give power-law fits to the data. These suggested laws can be used for testing hydrodynamical models of cometary atmospheres and for the interpretation of molecular observations, especially OH observations made with similar fields of views.
- The present results, compared to analyses of line shapes of parent molecules observed at millimetric wavelengths, yield significantly larger V_p 's. This may be attributed to the much larger field of view of the 18-cm observations. The two sets of data are complementary. The increase of V_p with the field of view demonstrates the acceleration of cometary gas with cometocentric distance.
- A threshold effect is observed: comets with small gas production rates (typically $Q_{\text{OH}} < \text{a few } 10^{28} \text{ s}^{-1}$)

have similar expansion velocities (typically $V_p \approx 0.8$ km s⁻¹). Gas acceleration is inefficient for such weak comets.

- Our results are in reasonable agreement with current hydrodynamical models of cometary atmospheres. Small discrepancies may be attributed to modelling issues such as inadequate treatment of the cooling/heating processes, or of the transitional region between hydrodynamical flow and free-molecular flow.

Acknowledgements. This work was done while W.-L. T. was guest of Observatoire de Paris. Part of her work was supported by NSC grant 94-2111-M-008-033 and Ministry of Education under the Aim for Top University Program NCU. The Nançay Radio Observatory is the Unité scientifique de Nançay of the Observatoire de Paris, associated as Unité de service et de recherche (USR) No B704 to the French Centre national de la recherche scientifique (CNRS). Its upgrade was financed jointly by the Conseil régional of the Région Centre in France, the CNRS and the Observatoire de Paris.

References

- Biver, N., Bockelée-Morvan, D., Colom, P., et al. 2002, *Earth Moon and Planets*, 90, 5
- Biver, N., Bockelée-Morvan, D., Crovisier, J., et al. 1999, *AJ*, 118, 1850
- Biver, N., Bockelée-Morvan, D., Crovisier, J., et al. 2000, *AJ*, 120, 1554
- Biver, N., Bockelée-Morvan, D., Crovisier, J., et al. 2006, *A&A*, 449, 1255
- Bockelée-Morvan, D., Colom, P., Crovisier, J., Gérard, E., & Bourgois, G. 1992, in *Asteroids, Comets, Meteors 1991*, 73–76
- Bockelée-Morvan, D. & Crovisier, J. 1987, in *ESA SP-278: Diversity and Similarity of Comets*, ed. E. J. Rolfe & B. Battrock, 235–240
- Bockelée-Morvan, D., Crovisier, J., & Gérard, E. 1990, *A&A*, 238, 382
- Bockelée-Morvan, D. & Gérard, E. 1984, *A&A*, 131, 111
- Bockelée-Morvan, D., Padman, R., Davies, J. K., & Crovisier, J. 1994, *Planet. Space Sci.*, 42, 655
- Budzien, S. A., Festou, M. C., & Feldman, P. D. 1994, *Icarus*, 107, 164
- Cochran, A. L. & Schleicher, D. G. 1993, *Icarus*, 105, 235
- Combi, M. R. & Delsemme, A. H. 1980, *ApJ*, 237, 633
- Combi, M. R., Harris, W. M., & Smyth, W. H. 2005, in *Comets II*, ed. M. C. Festou, H. U. Keller, & H. A. Weaver (Univ. Arizona Press), 523–552
- Combi, M. R., Kabin, K., Dezeew, D. L., Gombosi, T. I., & Powell, K. G. 1999, *Earth Moon and Planets*, 79, 275
- Crovisier, J. 1989, *A&A*, 213, 459
- Crovisier, J., Colom, P., Gérard, E., Bockelée-Morvan, D., & Bourgois, G. 2002a, *A&A*, 393, 1053
- Crovisier, J., Colom, P., Gérard, E., et al. 2002b, in *ESA SP-500: Asteroids, Comets, and Meteors: ACM 2002*, 685–688
- Despois, D., Crovisier, J., Bockelée-Morvan, D., Gérard, E., & Schraml, J. 1986, *A&A*, 160, L11
- Despois, D., Gérard, E., Crovisier, J., & Kazès, I. 1981, *A&A*, 99, 320
- Festou, M. C. 1981, *A&A*, 95, 69
- Gérard, E. 1990, *A&A*, 230, 489
- Harris, W. M., Scherb, F., Mierkiewicz, E., Oliverson, R., & Morgenthaler, J. 2002, *ApJ*, 578, 996
- Hodges, R. R. 1990, *Icarus*, 83, 410
- Ip, W.-H. 1983, *ApJ*, 264, 726
- Lämmerzahl, P., Krankowsky, D., Hodges, R. R., et al. 1987, *A&A*, 187, 169
- Lecacheux, A., Biver, N., Crovisier, J., et al. 2003, *A&A*, 402, L55
- Neufeld, D. A., Stauffer, J. R., Bergin, E. A., et al. 2000, *ApJ*, 539, L151
- Schloerb, F. P., Kinzel, W. M., Swade, D. A., & Irvine, W. M. 1987, *A&A*, 187, 475
- Tacconi-Garman, L. E., Schloerb, F. P., & Claussen, M. J. 1990, *ApJ*, 364, 672
- Tseng, W.-L. 2004, *Cometary water expansion velocity from OH line shapes*, Tech. rep., Nançay radio telescope
- van Driel, W., Pezzani, J., & Gérard, E. 1996, in *High-Sensitivity Radio Astronomy*, ed. N. Jackson & R. J. Davis (Cambridge Univ. Press), 229–232